Hindawi Publishing Corporation
International Journal of Antennas and Propagation
Volume 2007, Article ID 17426, 9 pages
doi:10.1155/2007/17426

Application Article

Localization and Tracking of Passive RFID Tags Based on Direction Estimation

Yimin Zhang, Moeness G. Amin, and Shashank Kaushik

Received 1 March 2007; Accepted 19 October 2007

Recommended by Hans-Erik Nilsson

Radio frequency identification (RFID) is poised for growth as businesses and governments explore applications implementing RFID. The RFID technology will continue to evolve to meet new demands for human and target location and tracking. In particular, there are increasing needs to locate and track multiple RFID-tagged items that are closely spaced. As a result, localization and tracking techniques with higher accuracy yet low implementation complexity are required. This paper examines the applicability of direction-of-arrival (DOA) estimation methods to the localization and tracking problems of passive RFID tags. Different scenarios of stationary and moving targets are considered. It is shown through performance analysis and simulation results that simple DOA estimation methods can be used to provide satisfactory localization performance.

1. INTRODUCTION

Radio frequency identification (RFID) is a very valuable business and technology tool for electronically identifying, locating, and tracking products, animals, and vehicles. RFID offers strategic advantages for businesses because it can track inventory in the supply chain more efficiently, provide real-time in-transit visibility, and monitor general enterprise assets. RFID also attracts pharmaceutical industry due to its increased anticounterfeit measures.

RFID tags can be either passive, semipassive (also known as semiactive), or active [1, 2]. Although all types use radio frequency energy to communicate between a tag and a reader, the method of powering the tags is different. An active RFID tag uses an internal power source (battery) within the tag to continuously power the tag and its RF communication circuitry, whereas a passive RFID tag has no internal power supply and relies on RF energy transferred from the reader to the tag. While this distinction may seem minor on the surface, its impact on the functionality of the system is significant. Passive and active tags have different communication ranges. From tag localization and tracking perspective, active tags (often referred to as beacons) broadcast their own signal and, therefore, are similar to any active sources. As a result, many existing localization and tracking methods can be readily applied. On the other hand, the fact that most passive tags are detected and identified by backscattering the carrier signal emitted from the reader makes the signal processing more complicated and challenging. In solving the localization and tracking problem, the backscattering signal from the tag can be detected only after sufficient suppression of the strong presence of forward signal from the reader as well as the scattered signal from the environment.

RFID tags open up a wide variety of applications. The main driving force behind the current RFID technologies remains logistics and supply chain applications. RFID techniques are also considered important in intelligent transportation system (ITS), health-care sectors, access control, and so forth. While some of these applications only require the acquisition of the RFID tags at certain check points, many applications demand or prefer to have the positioning information of the tags. For example, real-time positioning is critical in automatic item sorting in a warehouse, airplane baggage handling, and the different phases of transportation. The recent move by the pharmaceutical industry to track medications for anticounterfeiting medications may require even higher positioning accuracy.

Several important contributions have been made to the localization and tracking of RFID tags. LANDMARC is a well-known location sensing prototype system that improves the overall accuracy of locating objects by utilizing the concept of reference tags whose positions are known in priori [3]. In another experimental study, a mobile robot equipped with RFID antennas is tasked for determining the locations of RFID tags attached to objects in an indoor environment [4].

This paper examines the applicability of direction-of-arrival (DOA) estimation methods to the localization and tracking problems of passive RFID tags. Different scenarios with stationary and moving tags are considered. As a result of the anticollision algorithms that are commonly used in RFID readers, the DOA estimation is only required to process signals from a single tag at each time. This allows us to use a relatively simple structure of two antennas, and a rather complicated near-field DOA estimation problem with two variables (range and DOA) can be transformed into a range-independent single-variable (DOA) estimation problem. It is shown through performance analysis and simulation results that such simple DOA estimation methods can be used to provide satisfactory localization performance. In addition, the tracking problem of moving tags located on a conveyer belt is examined, and effective methods that utilize multiple frames of data and employ multiple sets of antenna arrays are considered.

2. ACTIVE AND PASSIVE RFID TAGS

While all types of RFID tags use radio frequency energy to communicate between a tag and a reader, the method of powering the tags is different. An active RFID uses an internal battery within the tag to continuously power the tag and its RF communication circuitry. As such, it only requires very low-level signals to be transmitted to the tag (because the reader does not need to power the tag), and the tag can generate high-level signals back to the reader, driven from its internal power source. Additionally, an active RFID tag is continuously powered, whether it is in the reader field or not. As discussed in the next section, these differences impact communication range, multitag collection capability, ability to add sensors and data logging, and many other functional parameters.

Passive RFID tags, on the other hand, have no internal power supply and, therefore, can be much smaller and have an unlimited life span. Most passive tags signal by backscattering the carrier signal received from the reader. Because passive tags are cheaper to manufacture and have no battery, the majority of RFID tags in existence are of the passive variety. Semipassive RFID tags are very similar to passive tags except for the addition of a small battery, which allows the tag IC to be constantly powered and removes the need for the antenna to be designed to collect power from the incoming signal. Antennas can therefore be optimized for the backscattering signal.

Although they both fall under the RFID moniker and are often discussed interchangeably, active RFID and passive RFID are fundamentally different technologies. While this distinction may seem minor on the surface, its impact on the functionality of the system is significant. Passive tags contain circuitry that gains power from radio waves emitted by readers in their vicinity. They use this power to reply their unique identifier to the reader. Therefore, passive RFID operation requires very strong signals from the reader, and the signal strength returned from the tag is constrained to very low levels by the limited energy. Active tags broadcast their own signal and may have longer range and larger memories than passive tags, as well as the ability to store additional information sent by the transceiver. To economize power consumption, many beacon concepts operate at fixed intervals.

From tag localization and tracking perspective, active RFID tags are similar to any other types of active sources. Therefore, many existing localization and tracking techniques can be applied. On the other hand, passive RFID tags require sufficient suppression of the signal from the reader and scattered signal from the environment to be performed before these methods can be applied. In this paper, we focus on the localization and tracking of passive tags.

3. COMMUNICATION PROCEDURES AND WAVEFORMS

When a reader and a tag communicate, the information can be sent either on the downlink (from reader to tag) or on the uplink (from tag to reader). There are three communication procedures that could be used by RFID systems: full duplex (FDX), half duplex (HDX), and sequential (SEQ). These different communication procedures are shown in detail in Figure 1 [1, 5]. With the FDX protocol, information can be sent on both the uplink and the downlink at the same time. For the HDX protocol, the communication alternates between the uplink and the downlink. Finally, for SEQ, the energy transfer from the transponder to the receiver pulsates at predetermined time periods. The uplink occurs between these pulses and the downlink occurs during the energy transfers.

In this paper, we consider EPCglobal Class I RFID tags operating in the UHF frequency band [6]. The operating frequency range in the United States is between 902 MHz and 928 MHz. The communications between a reader and a tag use the half-duplex protocol.

The reader communicates with tags using amplitude shift keying (ASK) with a minimum modulation depth of 30% and a maximum modulation depth of 100% (Figure 2(a)). Tags reply to reader commands with a backscattering modulation that follows a four-interval bit cell encoding scheme. As illustrated in Figure 2(b), two transitions are observed for a binary zero and four transitions are observed for a binary one during a bit cell [6]. The nominal data rate for tag to reader is twice the reader to tag rate but may vary up to 25% over an 80-bit response window due to oscillator drift in the tag.

4. DIRECTION-OF-ARRIVAL-BASED LOCALIZATION METHODS

4.1. Concept

Consider a localization problem of an RFID tag, as depicted in Figure 3. An array consisting of two reader antennas is used to perform the DOA-based localization. There is a region that both antennas can illuminate and receive backscattering signals from the tags.

We consider an idea channel environment where no multipath propagation is present. The effect of the forward signal from the reader and the environmental scattering is ignored

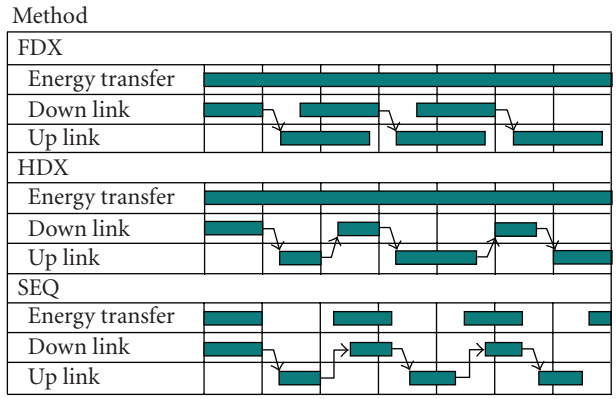

Figure 1: RFID communication procedures.

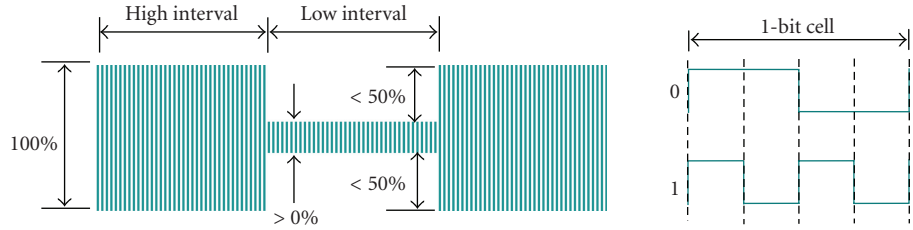

(a) Downlink (reader-to-tag) (b) Uplink (tag-to-reader)

Figure 2: RFID bit signal waveforms.

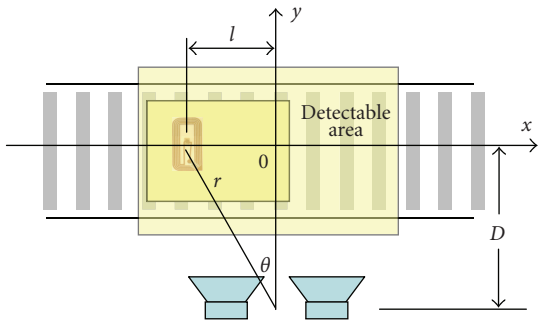

Figure 3: Geometry of the array structure.

in this section, and their removal is addressed in Section 4. As such, the performance of the tag DOA estimation is determined by the received signal-to-noise ratio (SNR), that is, the power ratio of the received backscattering ASK signal from the tag and the noise and the available data length. The latter depends on the class of tag.

It is noted that, when multiple tags are present, most anticollision algorithms perform a tree search. As a result, only the signals transmitted from a single tag will be successfully received at the reader without a collision problem. That is, for a collision-free data, only a single tag needs to be considered in the DOA estimation. Therefore, a two-sensor array has sufficient degrees of freedom (DOFs) to use MUSIC-like methods for the estimation of the signal and noise subspaces. More importantly, the DOA estimation problem can be simplified. In general, a near-field localization problem involves both the range and DOA as these two parameters are coupled [7]. For a near-field DOA estimation problem using a two-antenna array, however, it is shown in [8] and summarized below that the covariance matrix is independent of the range, thus the two-variable (range and DOA) problem is reduced into a single-variable (DOA) estimation problem. Furthermore, when only a single tag is active, the cross-correlation between the data received at the two antennas suffices to obtain the DOA estimation.

Let $\mathbf{x}(t) = [x_1(t), x_2(t)]^T$ be the received signal at the two antennas, where superscript ^{T} denotes vector transpose. Their baseband equivalent signals are expressed as

$$x_i(t) = \alpha_i s(t) \exp\left(-j\frac{2\pi}{\lambda}(r_i - r)\right) + n_i(t), \quad i = 1, 2, \quad (1)$$

where $s(t)$ is the signal received at the center of the array, which is considered as the phase center, and α_i is a real-valued factor representing different attenuation levels between the tag and the reader antennas. In addition, r_i is the distance between the ith antenna and the tag, r is the distance between the center of the array and the tag, λ is the wavelength at the hopping frequency over the observation period, and $n_i(t)$ is the additive white Gaussian noise at the ith antenna. The interelement spacing of the array, d, is chosen to satisfy $d \leq 0.5\lambda$. In practice, $d \ll r$ is satisfied and $r_i - r$ can be approximated as [8]

$$r_i - r = -\frac{(-1)^i d \sin(\theta)}{2} + \frac{d^2 \cos^2(\theta)}{8r}, \quad (2)$$

where θ is the DOA of the tag measured from the center of the array (see Figure 3).

Therefore, the phase difference ϕ between $x_1(t)$ and $x_2(t)$ becomes

$$\phi = \angle\{E[x_1^*(t)x_2(t)]\} = \frac{2\pi d}{\lambda}\sin(\theta), \tag{3}$$

where $*$ denotes complex conjugate, $E[\cdot]$ denotes the statistical expectation operation, and $\angle\{\cdot\}$ denotes the phase part of a complex value. In practice, the expectation operation can be replaced by the sample averaging over a period of time. For stationary tags, several blocks of RFID tag data (for EPCglobal class I RFID tag, each block contains 64 or 96 bits of tag information) can be incorporated to improve the DOA estimation performance.

When the phase difference ϕ between the two antennas is estimated as $\hat{\phi}$, the corresponding estimate of the DOA is

$$\hat{\theta} = \sin^{-1}\left(\frac{\lambda}{2\pi d}\hat{\phi}\right). \tag{4}$$

4.2. Moving tag tracking

For the tracking of moving tags, the length of the observation time period becomes important. This period depends on several factors, such as the moving speed, antenna beamwidth, communication protocol, multiplexing scheme between different sets of antennas, and whether there exist multiple tags. It is usually possible to receive tens of readings in each set of antennas.

Note that, in moving tag scenarios, the tags change their positions at different time instants (see Figure 4). Multiple reading results may be incorporated for the improvement of the tag tracking performance. In EPCglobal Class 1 RFID, the nominal tag-to-reader bit cell interval is 7.125 microseconds. Therefore, a 96-bit stream translates to 684 microseconds. For a typical value of the conveyer belt speed, the displacement of the tag over this period is small, and the tag can be considered stationary. For example, when the moving speed of the conveyer belt (and thus the tag) is $v = 5$ m/s, the displacement over the 684-microsecond period is 3.43 mm, which can be considered negligible. However, when multiple frames of data are used for tag tracking, the tag displacement over different frames, in general, has to be taken into account.

Refer to Figure 3, where D denotes the distance from the center of the two-antenna array to the conveyer belt, and l is location of the tag in the x-axis direction, using the center of the array as the reference. Then, the theoretical DOA, measured from the center of the array, is expressed as

$$\bar{\theta}(t) = \tan^{-1}\left(\frac{l(t)}{D}\right) = \tan^{-1}\left(\frac{l_0 - v\cdot(t - t_0)}{D}\right), \tag{5}$$

where l_0 is the position of the tag at a reference time instant t_0. Because v is known, l_0 at the reference time t_0 is the only parameter that determines the trace of the tag.

Therefore, when M observations are available in different time periods $t_1, t_2, \ldots, t_M$, we can obtain an improved estimate of l_0 from the following least-square fitting that utilizes the multiple observations (refer to Figure 5):

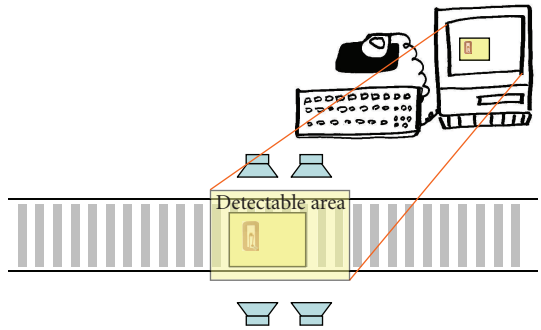

Figure 4: RFID-tagged item on a conveyer belt.

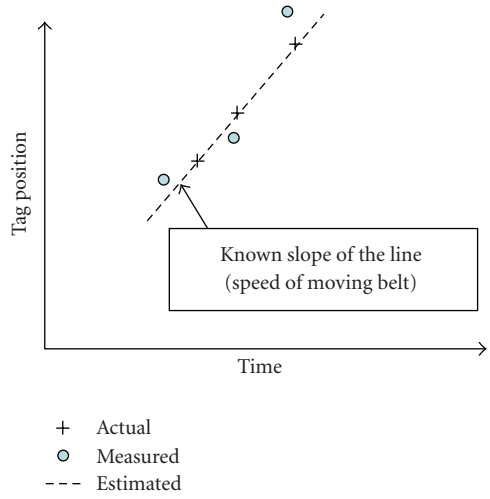

Figure 5: Illustration of the least-square method.

$$\begin{aligned} l_{0,\text{opt}} &= \operatorname{argmin}_{l_0}\sum_{i=1}^{M}\left|\hat{\theta}_i(t) - \bar{\theta}_i(t)\right|^2 \\ &= \operatorname{argmin}_{l_0}\sum_{i=1}^{M}\left|\sin^{-1}\left(\frac{\lambda}{2\pi d}\phi_i(t)\right) - \tan^{-1}\left(\frac{l_0 - v\cdot(t_i - t_0)}{D}\right)\right|^2. \end{aligned} \tag{6}$$

4.3. Performance analysis

The DOA estimation through the above operation is equivalent to performing the MUSIC algorithm to the received data [8]. The asymptotic MUSIC estimation error is extensively studied in [9, 10]. When N independent data samples are available, the variance of the DOA estimation, in terms of the spatial (radian) frequency, $\omega = (2\pi d/\lambda)\sin(\theta)$, is expressed as

$$\text{var}(\hat{\omega}) = \frac{1}{2N\xi}\cdot\frac{1}{h(\omega)}\left(1 + \frac{1}{2\xi}\right), \tag{7}$$

where ξ is the input SNR,

$$a = \left[\exp\left(-j\frac{2\pi}{\lambda}\left(\frac{d\sin(\theta)}{2}+\frac{d^2\cos^2(\theta)}{8r}\right)\right),\right.$$
$$\left.\exp\left(-j\frac{2\pi}{\lambda}\left(-\frac{d\sin(\theta)}{2}+\frac{d^2\cos^2(\theta)}{8r}\right)\right)\right]^T$$
$$= \exp\left[-j\frac{2\pi}{\lambda}\left(\frac{d\sin(\theta)}{2}+\frac{d^2\cos^2(\theta)}{8r}\right)\right][1,\exp(j\omega)]^T \tag{8}$$

is the steering vector, and

$$h(\omega) = \mathbf{d}^H\left(\mathbf{I}_2 - \frac{1}{2}\mathbf{a}\mathbf{a}^H\right)\mathbf{d}. \tag{9}$$

In the above equation, $\mathbf{I}_2$ is the 2×2 identity matrix and

$$\mathbf{d} = \frac{\partial \mathbf{a}}{\partial \omega}. \tag{10}$$

In the underlying two-antenna array case, it can be readily show that $h(\omega) = 1/2$. Therefore,

$$\mathrm{var}(\hat{\omega}) = \frac{1}{4N\xi}\left(1+\frac{1}{2\xi}\right) = \frac{1}{4N\xi}+\frac{1}{8N\xi^2}. \tag{11}$$

It is evident from this expression that, when the SNR is high, the variance of the DOA estimation is inversely proportional to the SNR, whereas it becomes inversely proportional to the square of the SNR when the input SNR is low. In [11], the importance of properly filtering the received signal for SNR enhancement, particularly for low SNR levels, is addressed. When a filter that matches the backscattering waveform is used, we can obtain L independent samples, where L is the number of bits transmitted from the tag in a single frame period. In this case, the SNR becomes

$$\xi = \frac{E_b}{N_0}, \tag{12}$$

with E_b denoting the bit energy, and N_0 denoting the noise spectrum density.

When M observation periods are available for least-square fitting in the moving tag tracking application, assuming that the variance at each observation period is equal, then the variance of the DOA estimation error becomes

$$\mathrm{var}(\hat{\omega}) = \frac{1}{4MN\xi}\left(1+\frac{1}{2\xi}\right). \tag{13}$$

In other words, the standard deviation of the DOA estimation error is reduced by a factor of $\sqrt{M}$. MN can be equivalently considered as the total number of available samples in the performance evaluation.

The input SNR depends on the reader and tag specifications as well as the service range. The analysis of the tag signal strength has been considered, for example, in [12, 13]. From the signal detection point of view, the SNR required for error-free detection of a sequence of 64 or 96 bits is about several decibels. The backscattering signals transmitted from a passive RFID tag are orthogonal in the signal subspace. Hence, the BER is given by [14]

$$\mathrm{BER} = \frac{1}{2}\mathrm{erfc}\left(\sqrt{\frac{E_b}{2N_0}}\right). \tag{14}$$

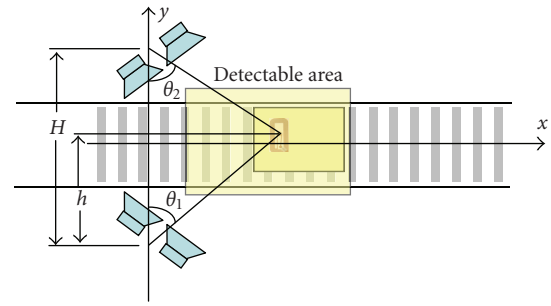

Figure 6: Tag localization using two oblique arrays.

Consider a relatively low value of SNR, $\xi = 5$ dB (which yields a BER of 3.8% for a tag signal), a 96-bit sequence will result in a DOA estimation variance of 0.001, or a standard deviation of $\sigma_\phi = 1.8^o$. When the interelement spacing is half-wavelength, it translates to $\sigma_\theta = 0.56^o$ when the tag is in the broadside direction of the array. With a two-meter range, it translates to a 2 cm standard deviation of the position error. As a result, the position error corresponding to $3\sigma_\theta$ is about 6 cm, within which the tag can be localized most of the time. When ten frames can be incorporated ($M = 10$), the standard deviation can be reduced to $\sigma_\theta = 0.17^o$, which translates to a 6 mm standard deviation of the position error and a 2 cm $3\sigma_\theta$ bound in the same two-meter range.

5. TAG LOCALIZATION USING TWO OBLIQUE ARRAYS

For the two-antenna array discussed so far, the range does not play a significant role in the phase difference between the two antennas [8]. Therefore, the DOA estimation provides the direction, but not the unique location of the RFID tag. In this section, we consider the use of two sets of two-antenna arrays, as shown in Figure 6. By using the same DOA estimation techniques at both arrays, such structure provides information of two oblique angles for accurate tag localization through triangulation. Note that a more accurate estimation of the tag location is possible through the use of near-field DOA estimation methods based on the observations of all four antennas (see, e.g., [7]). However, we consider that the triangulation-based approach is by far simpler.

Refer to Figure 6, we assume that the centers of the two arrays are, respectively, located at $(0, -H/2)$ and $(0, H/2)$. The estimated DOAs of the tag by the two arrays are denoted

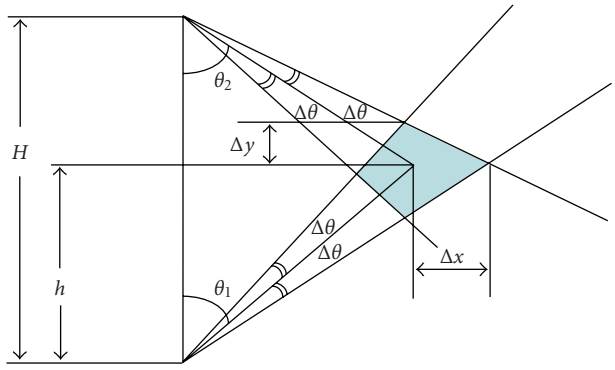

Figure 7: Geometry for localization error analysis.

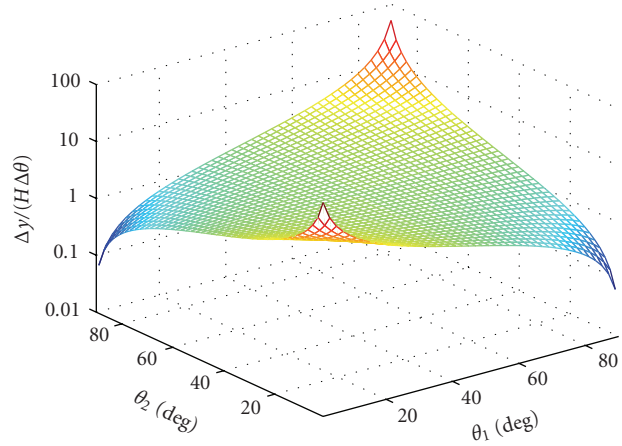

Figure 8: Localization error in the y direction.

as θ_1 and θ_2. Then, the estimated position of the tag is expressed as

$$x_e = H \cdot \frac{\tan(\theta_1)\tan(\theta_2)}{\tan(\theta_1) + \tan(\theta_2)},$$
$$y_e = \frac{H}{2} \cdot \frac{\tan(\theta_2) - \tan(\theta_1)}{\tan(\theta_1) + \tan(\theta_2)}, \quad (15)$$

where H is the distance between the centers of the two arrays.

To consider the impact of DOA estimation error on the accuracy of the location estimation, we consider the geometry illustrated in Figure 7. The errors in the x and y directions, corresponding to $\Delta\theta$ in both DOA estimates, are obtained as

$$\Delta x = H\Delta\theta,$$
$$\Delta y = H\Delta\theta \cdot \frac{\sin(2\theta_1) + \sin(2\theta_2)}{2\sin^2(\theta_1 + \theta_2)}. \quad (16)$$

Interestingly, the error in the x direction is a function of only H and $\Delta\theta$, and is independent of the tag position. On the other hand, the error in the y direction is more complicated. As shown in Figure 8, Δy assumes a high value along $\theta_1 = \theta_2$ where $\Delta y = H\Delta\theta/\sin(2\theta_1)$, particularly when both of them are close either to 0 or 90°. On the other hand, it takes a small value when $\theta_1 + \theta_2 = 90°$, where $\Delta y = H\Delta\theta \cdot \sin(2\theta_1)$. That is, to achieve a high localization accuracy in the y direction, it is desirable to place the tag off the center. In particular, when either θ_1 or θ_2 equals to 45°, $\Delta y = H\Delta\theta$.

As a design guidance, therefore, the two arrays should be spaced as close as possible to minimize the error in both x and y directions. In addition, if the y direction error is a concern, the detectable area should be set around $x = H/2$ so that the worst error is minimized.

6. SIMULATION RESULTS

To verify the DOA estimation performance of the RFID tags and confirm the effectiveness of exploiting signal oversampling as well as least-square fitting schemes, simulation experiments are performed. The block diagram of the simulated system environment is illustrated in Figure 9. Consider the uplink interval, the reader transmits frequency-hopping

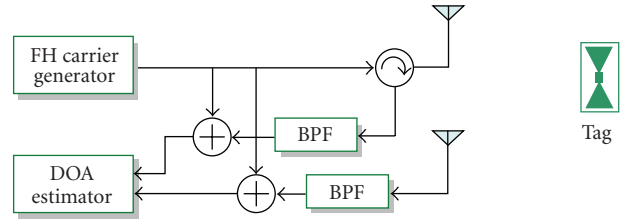

Figure 9: Block diagram of the simulated environment.

(FH) carrier signal, whereas the tag replies with the information message in the backscattering manner. The carrier signal component is coherently subtracted from the received signals, and the results are used to perform DOA estimation.

6.1. Signal model

The signal received at an antenna is expressed as

$$y_i(t) = [\beta_i + \gamma_i(t)]u(t) + \alpha_i s(t)\exp\left(j\frac{(-1)^i \pi d}{\lambda}\sin[\theta_i(t)]\right) + n_i(t), \quad i = 1, 2, \quad (17)$$

where $u(t) = \exp(2\pi f_c t)$ is the FH carrier waveform transmitted from the reader with varying frequency f_c, β_i is a complex scalar representing the strength of the carrier waveform, depending on several factors including whether the antenna is used for transmission, the performance of the circulator, and the distance between the antennas. $\gamma_i(t)$ represents the slowly time-varying coefficient of the environment scattering of the forward signal. $s(t)$ is the uplink signal with a Manchester-like envelope, as shown in Figure 2(b), and α_i is a real-valued scalar, representing the strength of the return signal from the tag. Moreover, $n_i(t)$ denotes the noise term.

For information bits 0 and 1, the respective waveforms of $s(t)$ are expressed as

$$s_0(t) = \begin{cases} \exp(j2\pi f_c t), & 0 \le t \le \dfrac{T}{2}, \\ -\exp(j2\pi f_c t), & \dfrac{T}{2} \le t \le T, \end{cases}$$

$$s_1(t) = \begin{cases} \exp(j2\pi f_c t), & 0 \le t \le \dfrac{T}{4}, \ \dfrac{T}{2} \le t \le \dfrac{3T}{4}, \\ -\exp(j2\pi f_c t), & \dfrac{T}{4} \le t \le \dfrac{T}{2}, \ \dfrac{T}{3} \le t \le T. \end{cases} \tag{18}$$

The carrier waveform components as well as the environmental scattering, that is, the first term on the right-hand side of (17), have a high power but occupy only a very narrow frequency band around the carrier frequency. As a result, they can be eliminated from the received signal through proper filtering, provided that the receiver has high dynamic range and robust carrier frequency. Because of the symmetric signaling structure of the Manchester signaling, it is uncorrelated to the carrier signal, regardless of the value of the information bit from the tag. As the result, we can obtain the following signal after the suppression of the carrier signal and environmental noise:

$$x_i(t) = \alpha_i s(t) \exp\left(j \frac{(-1)^i \pi d}{\lambda} \sin[\theta_i(t)]\right) + n_i(t), \tag{19}$$

Note that (19) is exactly the same as (1). It is emphasized that, in the above equation, the noise term not only includes the equivalent thermal noise, but may also include other distorting factors such as the quantization noise, and the residual error of the carrier waveform suppression. Because the uplink signal from the tag is very weak, all these distorting factors may appear as significant sources that limit the achievable SNR.

6.2. Localization of stationary tags

In the simulations, the carrier signal transmitted from reader and backscattering signal transmitted from a tag are generated. The carrier frequency is 910 MHz, and a sampling rate of 5 GHz is used. The interelement spacing is set to be half wavelength with respect to the center of the 902–928 MHz band, that is, 915 MHz. The signal power of the backscattering signal is set to be 70 dB lower than that of the carrier signal as measured at the reader antennas [15]. As described in Section 6.1, the carrier signal component is subtracted and the resulting signal is filtered using the matched filter. The E_b/N_0 value is evaluated as the ratio between the energy of the tag signal and the additive noise spectrum. We use one frame of tag signal for the DOA estimation, and one sample is used for each bit interval and. As a result, 96 samples are used to estimate the phase difference between the two receive antennas.

Figure 10 shows the standard deviation (STD) of the error of the DOA (σ_θ) versus the input E_b/N_0. Each result is evaluated using 100 independent trials. The simulation results well coincide with the theoretical results.

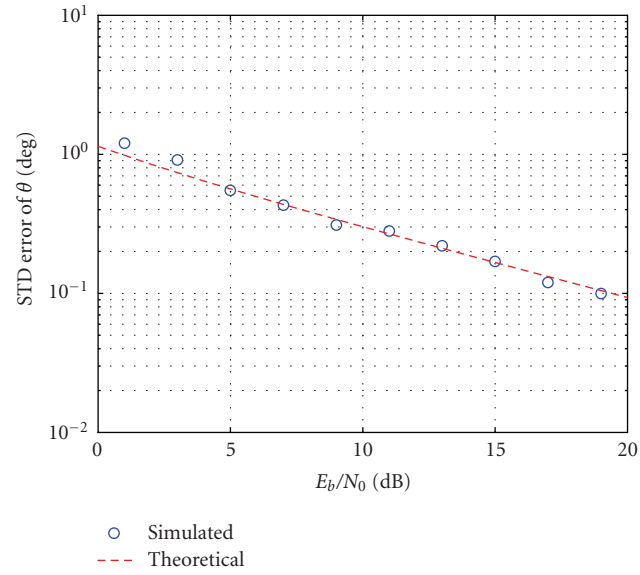

Figure 10: Standard deviation of DOA estimation error (stationary tag, single frame).

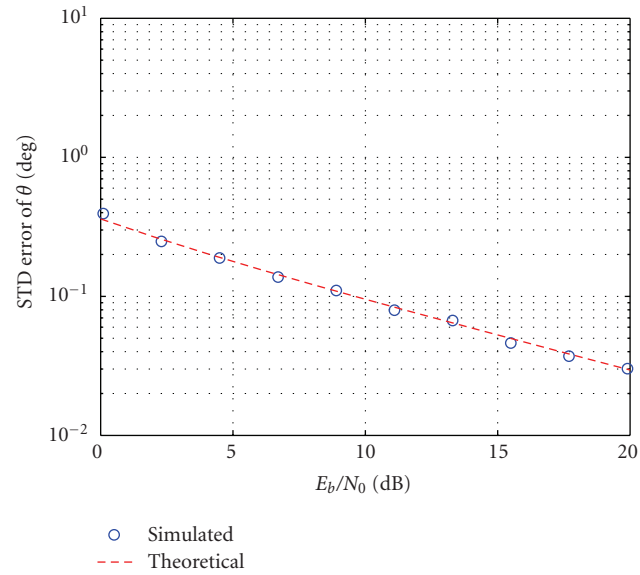

Figure 11: Standard deviation of DOA estimation error (stationary tag, $M = 10$).

As we discussed earlier, incorporating observed data from multiple frames can improve the DOA estimation accuracy. Figure 11 shows the results when ten frames are incorporated.

6.3. Effect of least-square fitting in moving tag tracking

To consider the tracking of a moving tag, we let the tag to move from position $l = -0.5$ meter to $l = 0.5$ meter, with a step size of $\Delta l = 0.1$ meter. The distance from the array center to the conveyer is $D = 2.0$ meter. The input SNR is set

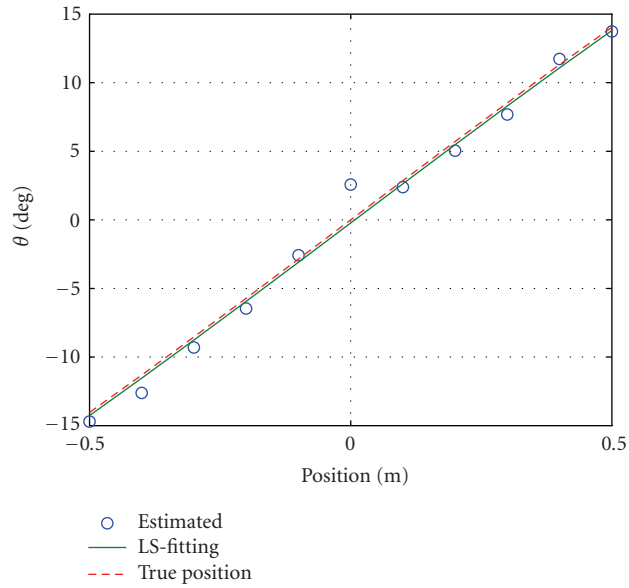

Figure 12: Estimation performance of a moving tag at the 11 positions.

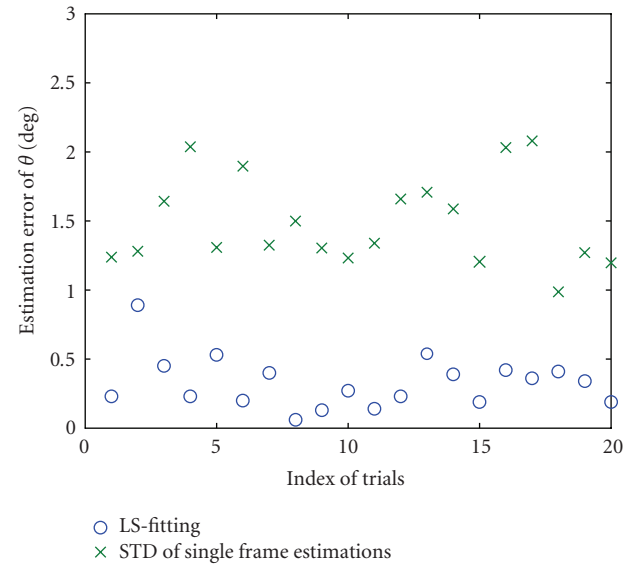

Figure 13: Comparison of the DOA estimation error (20 trials).

to $E_b/N_0 = 5$ dB. A single measurement over the 11 positions and the least-square fitting result are shown in Figure 12 with the true positions of the tags. The root square error of the 11 individual measurements is 1.05°, whereas the error of the least-fitting mean value becomes 0.23°. Figure 13 compares the estimation error results over 20 independent trials. The performance improvement by using the least-square fitting to incorporating multiple tag positions is evident.

7. CONCLUSIONS

In this paper, we have examined the applicability of a two-antenna array structure for the localization and tracking of passive RFID tags. By simply comparing the phase of the matched filtered output at each bit interval, it has been demonstrated through analysis and simulation experiments that it achieves high DOA estimation accuracy for the localization and tracking of closely spaced items. In addition, incorporating observations over multiple frames or multiple positions can significantly improve the DOA estimation performance. We have also considered the use of two oblique arrays for triangulation-based tag localization, and a guidance for array configuration design is provided.

ACKNOWLEDGMENTS

This work was supported in part by the Ben Franklin Technology Partners of Southeastern Pennsylvania. Parts of this work were presented in SPIE Symposium on Defense and Security (Orlando, Fla, USA), April 2006.

REFERENCES

[1] K. Finkenzeller, *RFID Handbook*, John Wiley & Sons, New York, NY, USA, 2nd edition, 2003.

[2] Savi Technology White Paper, "Active and passive RFID: two distinct, but complementary, technologies for real-time supply chain visibility," http://www.autoid.org/2002_Documents/sc31_wg4/docs_501-520/520_18000-7_WhitePaper.pdf.

[3] L. M. Ni, Y. Liu, Y. C. Lau, and A. P. Patil, "LANDMARC: indoor location sensing using active RFID," in *Proceedings of the 1st IEEE International Conference on Pervasive Computing and Communications (PerCom '03)*, pp. 407–415, Dallas-Fort Worth, Tex, USA, March 2003.

[4] D. Hähnel, W. Burgard, D. Fox, K. Fishkin, and M. Philipose, "Mapping and localization with RFID technology," Intel White Paper IRS-TR-03-014, December 2003, http://www.intel-research.net/Publications/Seattle/012020041250_211.pdf.

[5] Tektronix Technical Brief, "Radio frequency identification (RFID) overview," http://www2.tek.com/cmswpt/tidetails.lotr?ct=TI&cs=Technical+Brief&ci=2254&lc=EN.

[6] "860MHz—930MHz Class I Radio Frequency Identification Tag Radio Frequency & Logical Communication Interface Specification Candidate Recommendation, Version 1.0.1," Tech. Rep., Auto-ID Center, November 2002, http://www2.tek.com/cmswpt/tidetails.lotr?ct=TI&cs=Technical+Brief&ci=2254&lc=EN.

[7] B. A. Obeidat, Y. Zhang, and M. G. Amin, "Range and DOA estimation of polarized near-field signals using fourth-order statistics," in *Proceedings of the IEEE International Conference on Acoustics, Speech and Signal Processing (ICASSP '04)*, vol. 2, pp. 97–100, 2004.

[8] J. Wang, M. Amin, and Y. Zhang, "Signal and array processing techniques for RFID readers," in *Wireless Sensing and Processing*, vol. 6248 of *Proceedings of SPIE*, Orlando, Fla, USA, April 2006.

[9] P. Stoica and A. Nehorai, "MUSIC, maximum likelihood, and Cramer-Rao bound," *IEEE Transactions on Acoustics, Speech, and Signal Processing*, vol. 37, no. 5, pp. 720–741, 1989.

[10] P. Stoica and A. Nehorai, "MUSIC, maximum likelihood, and Cramer-Rao bound: further results and comparisons," *IEEE Transactions on Acoustics, Speech, and Signal Processing*, vol. 38, no. 12, pp. 2140–2150, 1990.

[11] W. Mu, Y. Zhang, and M. Amin, "A subband MUSIC technique for direction finding," in *Proceedings of the IEEE/Sarnoff Symposium on Advances in Wired and Wireless Communications*, Trenton, NJ, USA, March 1999.

[12] Y. Han, Q. Li, and H. Min, "System modeling and simulation of RFID," in *Auto-ID Labs Research Workshop*, Zurich, Switzerland, 2004.

[13] D. M. Dobkin, *The RF in RFID: Passive UHF RFID in Practice*, Newnes, Burlington, Mass, USA, 2008.

[14] S. Haykin, *Communication Systems*, John Wiley & Sons, New York, NY, USA, 4th edition, 2001.

[15] "RFID: Physics of backscatter tags," NCR Report, http://www5.ncr.com/it/products/pdf/sa_backscatterwp.pdf.

AUTHOR CONTACT INFORMATION

Yimin Zhang: Radio Frequency Identification (RFID) Laboratory, Center for Advanced Communications, Villanova University, Villanova, PA 19085, USA; yimin@ieee.org

Moeness G. Amin: Radio Frequency Identification (RFID) Laboratory, Center for Advanced Communications, Villanova University, Villanova, PA 19085, USA; moeness.amin@villanova.edu

Shashank Kaushik: Radio Frequency Identification (RFID) Laboratory, Center for Advanced Communications, Villanova University, Villanova, PA 19085, USA; shashank.kaushik@villanova.edu